Talanta 129 (2014) 100–105

Contents lists available at ScienceDirect

Talanta

journal homepage: www.elsevier.com/locate/talanta

Construction of an electrochemical sensor based on amino-functionalized metal-organic frameworks for differential pulse anodic stripping voltammetric determination of lead

Yang Wang*, Huali Ge, Yichun Wu, Guiqin Ye, Huanhuan Chen, Xiaoya Hu*

College of Chemistry and Chemical Engineering, Yangzhou University, Yangzhou 225002, China

A R T I C L E I N F O

Article history:
Received 13 March 2014
Received in revised form
6 May 2014
Accepted 10 May 2014
Available online 17 May 2014

Keywords:
Amino-functionalization
Metal-organic frameworks
Differential pulse anodic stripping voltammetry
Lead

A B S T R A C T

Metal-organic frameworks composite materials have received tremendous attention because of their versatile structures and tunable porosity for various applications. Herein, amino-functionalized metal-organic frameworks (NH_2–$Cu_3(BTC)_2$; BTC=benzene-1,3,5-tricarboxylate) was prepared and used as a novel electrode modifier for the determination of trace levels of lead. NH_2–$Cu_3(BTC)_2$ shows quite a good capability for the efficient adsorption of lead from aqueous solutions. The parameters affecting the electrochemical process, such as electrolyte solution pH, the amount of NH_2–$Cu_3(BTC)_2$ suspension, accumulation potential and accumulation time, were investigated in detail. Under the optimal conditions, the electrochemical sensor exhibited a linear response to the concentration of lead in the range of 1.0×10^{-8}–5.0×10^{-7} mol L^{-1} ($R^2=0.9951$) with a detection limit of 5.0×10^{-9} mol L^{-1}. The relative standard deviation of 11 successive scans was 3.10% for 1.0×10^{-8} mol L^{-1} lead. The method was validated with certified reference material (stream sediment and milk powder) and the analytical results coincided well with the certified values. Furthermore, the method was successfully applied to the determination of target analytes in tap and lake water samples and good recoveries were obtained from different spiked values.

1. Introduction

Lead is a neurotoxic metallic element that can be absorbed by the body and accumulated in bloods and bones. Excess intake poses an important threat to human health. In particular, it can decrease intelligence and slower neurological and then strongly affects the mental and physical development of children [1,2]. The determination of lead has been carried out with various detection techniques such as electrothermal atomic absorption spectrometry [3], atomic fluorescence spectrometry [4], inductively coupled plasma optical emission spectrometry [5] and electrochemical methods [6,7]. In comparison with other methods, electrochemical methods have attracted greater attention in the last two decades due to their low cost, high sensitivity, easy operation and the ability of analyzing element speciation.

Nowadays, most electrochemical methods are based on the use of modified electrodes, because they exhibit enhanced performance by incorporating the chemistry and physics of the immobilized species. Among the large variety of chemically modified electrodes, chitosan gold nanocomposite [8], silver nanoparticles [9], bismuth film [10], stannum film [11], stannum/bismuth/poly(p-aminobenzene sulfonic acid) film [12], and bismuth-dispersed xerogel-based composite films [13] have been successfully employed as electrode coatings, providing effective electrochemical gates for the detection of analytes such as lead, zinc, cadmium, tin and mercury. Moreover, the potential of amino group functionalized based electrodes have also been explored as versatile electrode modifiers [14–16].

Metal-organic frameworks (MOFs) are crystalline porous coordination polymers that can be characterized as infinite 1D, 2D, or 3D networks resulting from the combination of metal species and organic linkers. A well-known MOFs is $Cu_3(BTC)_2$ (BTC=benzene-1,3,5-tricarboxylate), which is formed by paddlewheel secondary building units containing Cu^{2+} dimers coordinatively linked to carboxylic oxygen atoms from organic benzene-1,3,5-tricarboxylate (BTC) ligands [17,18]. Due to large porosity and high surface area, $Cu_3(BTC)_2$ offers unprecedented opportunities in gas-storage, catalysis, and small molecule sensing. Moreover, development of MOFs based composite for the electrochemical field of interest is becoming increasing. For instance, Copper (II)-based MOFs were used as selective electrocatalysts for the reduction of O_2 and CO_2

---

* Corresponding authors. Tel./fax: +86 514 87975587.
E-mail addresses: wangyzu@126.com (Y. Wang), xyhu@yzu.edu.cn (X. Hu).

http://dx.doi.org/10.1016/j.talanta.2014.05.014
0039-9140/© 2014 Elsevier B.V. All rights reserved.

[19,20]. Recent reports suggested that Au–SH–SiO_2 nanoparticles supported on MOF was utilized as a sensor for electrocatalytic oxidation and determination of hydrazine and L-cysteine [21,22].

In this paper, amino-functionalized $Cu_3(BTC)_2$ composite materials were fabricated as a novel electrode modifier. The electrochemical sensing performance was evaluated for lead sensor, and this new electrode displayed well-defined, sharp and highly reproducible stripping peaks at low concentrations of lead. Various parameters related to the measurement procedure were investigated and optimized to allow the resulting sensors to use in the analysis of real samples.

2. Experimental section

2.1. Apparatus

A CHI660A electrochemical workstation (Chenhua Instrument, Shanghai, China) was used for voltammetric measurements with a three-electrode system. The working electrode was the NH_2–$Cu_3(BTC)_2$ modified glassy carbon electrode (GCE). The counter electrode was a platinum wire and the reference electrode was an Ag/AgCl electrode. X-ray diffraction (XRD) patterns were recorded on a D8 Advance X-ray diffractometer (Bruker Co., Germany) at room temperature. Field emission scanning electron micrographs (SEM) were obtained with a Hitachi S-4800 microscope (Japan) at an acceleration voltage of 15 kV. Thermogravimetric analysis (TGA) was performed by means of a Pyris 1 TGA (PerkinElmer, America), under N_2 at a scan rate of 10 °C min^{-1}.

2.2. Reagents and materials

A 1.0×10^{-2} mol L^{-1} lead stock solution was prepared by dissolving 3.312 g $Pb(NO_3)_2$ (Jinshan chemicals, Shanghai, China) in 100 mL 1% (v/v) nitric acid. Working standard solutions were obtained by step-wise dilution. Copper (II) nitrate trihydrate ($Cu(NO_3)_2 \cdot 3H_2O$), 1,3,5-benzene tricarboxylic acid (H_3BTC), *N,N*-dimethylformamide (DMF), 2-amino-1,4-benzenedicarboxylate (ABDC), ethanol and chloroform in this work were at least of analytical reagent grade without further purification and were obtained from Sinopharm Chemical Reagent Co., Ltd. unless otherwise stated. Double de-ionized water (18 MΩ cm) was used throughout the experiments. Reference materials stream sediment and milk power were purchased from the BHH Biotechnology Co., Ltd. Nitrogen gas (99.999%) was used for purging oxygen in a solution to provide an inert atmosphere.

2.3. MOFs synthesis

NH_2–$Cu_3(BTC)_2$ was synthesized based on a previous literature after a minor modification [23]: Briefly, copper (II) nitrate trihydrate (12.2 g), H_3BTC (5.8 g), ABDC (1.8 g) were dissolved in a beaker containing DMF (85 mL), de-ionized water (85 mL) and ethanol (85 mL) under magnetic stirring for 30 min, and then heated in a Teflon lined steel autoclave at 85 °C for 24 h. After cooling to ambient temperature, the sky-blue crystals was filtered, washed with DMF and ethanol, and immersed in chloroform, which was decanted and replaced with fresh chloroform two times over three days. The final products were heated at 130 °C for 3 days before use.

2.4. Fabrication of NH_2–$Cu_3(BTC)_2$ modified electrode

NH_2–$Cu_3(BTC)_2$ (1 mg) was dispersed in 1 mL DMF and the mixture was agitated in an ultrasonic bath for one hour to achieve a well-dispersed suspension. Prior to use, the bare GCE was polished to a mirror-like surface with 0.05 μm α-Al_2O_3, then rinsed ultrasonically with water and absolute ethanol and sonicated in de-ionized water. A drop of this dispersion with the volume of 5 μL was coated on the surface of the GCE, and the NH_2–$Cu_3(BTC)_2$ composite modified electrode was obtained after it was dried in air for approximately 4 h.

2.5. Sensing procedure

In order to get the high sensitivity of detection, anodic stripping voltammetric technique was used and performed in a 10 mL electrochemical cell, if not stated otherwise, containing appropriate amounts of lead and 0.1 mol L^{-1} of acetate buffer solution (pH=4.5). The preconcentration was carried out at −1.0 V for 300 s under stirring and after a 10 s equilibration period, the voltammogram was recorded by applying a positive-going differential pulse stripping voltammetric potential scan from −1.0 to −0.1 V with a step potential of 10 mV, pulse amplitude of 100 mV and pulse width of 1.0 s. All potentials were referred to the Ag/AgCl reference electrode. The calibration curve was obtained by plotting the peak current versus the lead concentration.

3. Results and discussion

3.1. Characterization studies

The crystal structure and phase purity of the as-synthesized MOFs were characterized by XRD. All the diffraction peaks of the samples can be indexed to those of the highly quality $Cu_3(BTC)_2$ reported in the literature [18], and no obvious peaks of impurities can be detected in these XRD patterns. As shown in Fig. 1a, the nine major peaks found at 7.78°, 11.73°, 13.34°, 14.72°, 19.16°, 20.28°, 22.31°, 26.11° and 29.44° on the 2θ scale correspond respectively to the (200), (220), (222), (400), (331), (440), (600), (731) and (751) crystal planes. By comparing the XRD of NH_2–$Cu_3(BTC)_2$ and $Cu_3(BTC)_2$, we may safely draw the conclusion that the presence of –NH_2 functional group in the MOFs structure has not any effect on the XRD spectrum, indicating that increased amino did not change the metal ions and carboxylic acid organic ligand structure.

Thermogravimetric analysis (TGA) of NH_2–$Cu_3(BTC)_2$ is presented in Fig. 1b. The sample shows a little weight loss between 23.11 and 121.38 °C, which is ascribed to the removal of H_2O molecules and C_2H_5OH molecules present in the channels and coordinated to the metal centers of the MOF-structure. At temperatures between 121.38 and 288.73 °C, 7.4% of the weight was lost in NH_2–Cu_3 $(BTC)_2$, due to the displacement of the coordinated DMF molecules. All guest molecules can be removed at 288.73 °C. A third large weight change was observed from 289.51 to 596.20 °C. After decomposition at 350 °C, c.a. 35.6% of the starting weight remains, and this residual material could correspond to the formation of copper oxides and metallic copper. Hence, the obtained electrode modifier is stable at the current operating temperature.

The SEM image for the microstructures of the $Cu_3(BTC)_2$ is presented in Fig. 2, which was obtained as cube-shaped crystals with a smooth surface, demonstrating the good crystallinity of the material. In contrast, the crystal surface texture of NH_2–$Cu_3(BTC)_2$ was changed dramatically and flocculent substances appeared in the surface. These images were similar to the previous reports [24,25].This may be caused by impurities or a second phase nucleating on the surface of the crystals. That is, the Cu–BDC started to nucleate on the surface of the crystals when the reaction between BDC and Cu salt to make the Cu–BDC is performed at a lower temperature.

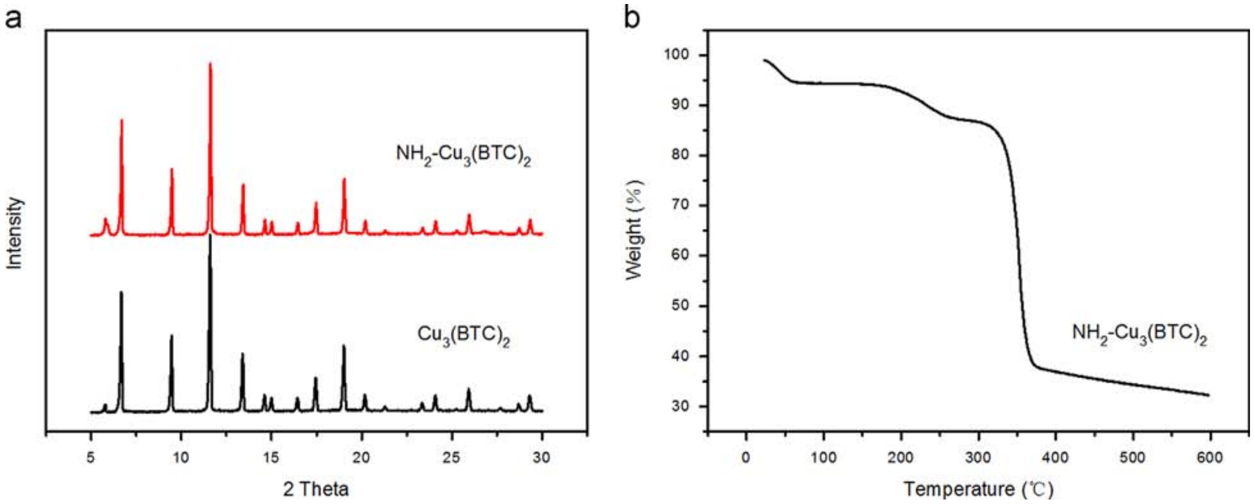

Fig. 1. (a) Powder X-ray diffraction patterns of $Cu_3(BTC)_2$ and NH_2-$Cu_3(BTC)_2$. (b) Thermogravimetric analysis of NH_2–$Cu_3(BTC)_2$.

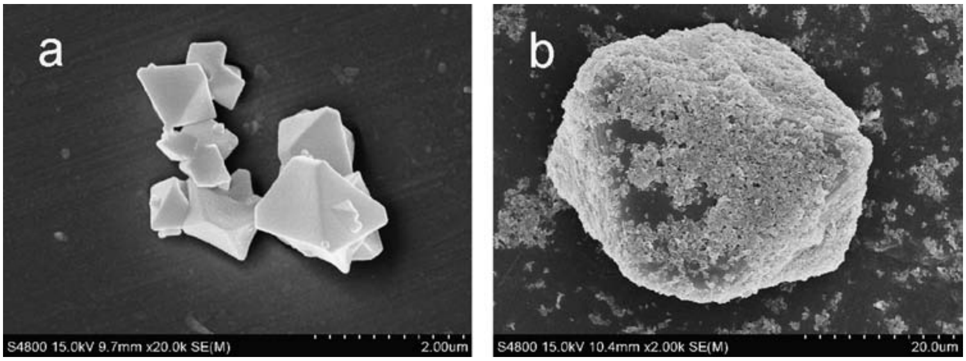

Fig. 2. SEM images of $Cu_3(BTC)_2$ (a) and NH_2–$Cu_3(BTC)_2$ (b).

Modification of GCE with a NH_2–$Cu_3(BTC)_2$ composite material contributes to a strong accumulation of lead ions from the solution phase onto the surface of the modified electrode under open circuit conditions. Fig. 3 shows the differential pulse voltammograms of 1.0×10^{-7} mol L^{-1} lead at the bare GCE (curve a), $Cu_3(BTC)_2$/GCE (curve b) and NH_2–$Cu_3(BTC)_2$/GCE (curve c) after 300 s accumulation. Three GCEs showed very different sensitivities. The response on the bare GCE was almost not detectable (curve a). With the same conditions, the $Cu_3(BTC)_2$ modified GCE (curve b) gave a signal at -0.525 V because of the absorbing effect of the $Cu_3(BTC)_2$, while a remarkable increase in response signal was observed on the NH_2–$Cu_3(BTC)_2$ modified GCE (curve c). This clearly demonstrates the favorable signal-enhancing effect of the NH_2–$Cu_3(BTC)_2$. The proposed mechanism of the stripping voltammetric measurement is the following. First, lead ions were accumulated from the solution phase onto the surface of the NH_2–$Cu_3(BTC)_2$/GCE by selective complexation with free functional amino group to result in the formation of a metal–ligand complex, and then the complexed ions accumulated in the modifying layer were reduced by applying a constant voltage of -0.9 V in accumulation. Lead is then electrochemically stripped back into the solution by scanning toward positive potential using the differential pulse voltammetric method. Second, lead ions can penetrate into the $Cu_3(BTC)_2$ channels, and the shape and size of the pores lead to shape- and size-selectivity over the metal ions which may be accumulated. The synergistic combinations of these effects lead to a greater amount of lead accumulation on the surface of NH_2–$Cu_3(BTC)_2$/GCE. Since lead peak current is dependent on the concentration of lead in the accumulation solution, this can be applied to the quantification of different levels of lead ions. The effect of NH_2–BDC linker concentration was examined using a concentration range from 10 to 50% in the ligands, and the oxidation peak current reached maximum at a concentration of 25%. So glassy carbon electrode modified with

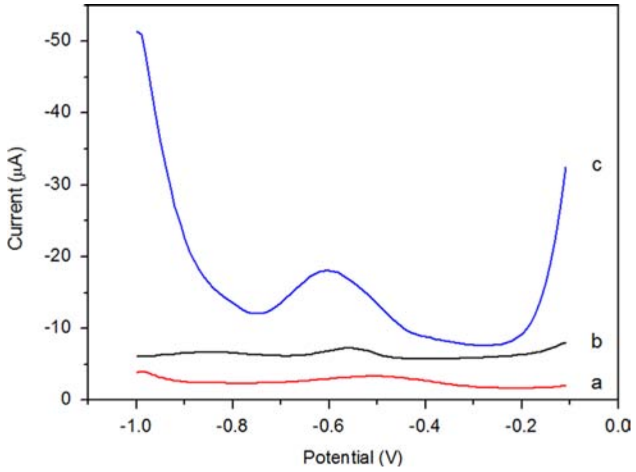

Fig. 3. Differential pulse voltammograms of 1.0×10^{-7} mol L^{-1} of lead in acetate buffer solution (pH 4.5) at bare GCE (a), $Cu_3(BTC)_2$/GCE (b) and NH_2–$Cu_3(BTC)_2$/GCE (c).

NH_2–$Cu_3(BTC)_2$ by 25% NH_2–BDC linker was used for further studies.

3.2. Optimization of experimental conditions

In order to establish the most suitable experimental conditions for the differential pulse anodic stripping voltammetric measurement of 1.0×10^{-7} mol L^{-1} lead at NH_2–$Cu_3(BTC)_2$/GCE in acetate buffer solution, a univariate optimization study was performed with the pH of measure solution, the amount of NH_2–$Cu_3(BTC)_2$ suspension, the accumulation potential and the accumulation time.

The influence of pH on the response of lead has been investigated in the pH range from 3.0 to 5.5. The acidity of a solution has two effects on metal adsorption. First, protons in acid solution can protonate binding sites of the chelating molecules. Second, hydroxide in basic solution may complex and precipitate metal ions. Therefore, the pH of a solution is the first parameter to be optimized. The effect of pH on lead adsorption was showed in Fig. 4a. It was noted that the current increased with increasing pH at around pH 3–4.5. A further increase of the pH led to a decline of the current. These observations might be explained as follows: at low pH, the signal intensity of lead was low, which was due to the protonated amino groups repulsing with the cations via electrostatic repulsion. With the increase of pH, the protonated amino groups decreased, and electrostatic attraction resulted in a higher stripping current of lead. The best signal intensity was reached at pH 4.5. In addition, the hydrolysis degree of the metal ions increases along with the increasing of pH, and white $Pb(OH)_2$ precipitate was formed. Then pH 4.5 was chosen for further studies.

According to the aforementioned results, introducing the NH_2–$Cu_3(BTC)_2$ on the surface of the GCE caused a considerable enhancement in the electrochemical behaviors of lead. This reveals that the amount of NH_2–$Cu_3(BTC)_2$ has a predominant role in the voltammetric response of lead. The amounts of 2, 3, 4, 5, 6 and 7 μL of NH_2–$Cu_3(BTC)_2$ suspension (1 mg mL^{-1}) were investigated. The results showed that the oxidation peak current of lead increased quickly through increasing the volume of NH_2–$Cu_3(BTC)_2$ suspension deposited on the surface of GCE up to 5 μL (Fig. 4b). Further increase, caused a reduction in the anodic peak current of lead. This can arise from larger film thickness, which caused increasing resistance of the film modifier against the electron transfer and sluggish mass transfer process for lead. As a result, 5 μL of 1 mg mL^{-1} NH_2–$Cu_3(BTC)_2$ suspension was selected as optimum volume.

An accumulation step is usually a simple and effective way to enhance the sensitivity of the voltammetric determinations. The effect of accumulation potential on the stripping peak currents of lead over the potential range from −0.8 to −1.2 V was explored (Fig. 4c). When accumulation potentials were more negative than −1.0 V, some other chemicals may be reduced at these potentials and interfere with the determination; while the potentials were more positive than −1.0 V, the background current became higher. Therefore, for further study, accumulation potential of −1.0 V was recommended. Furthermore, the effect of the accumulation time

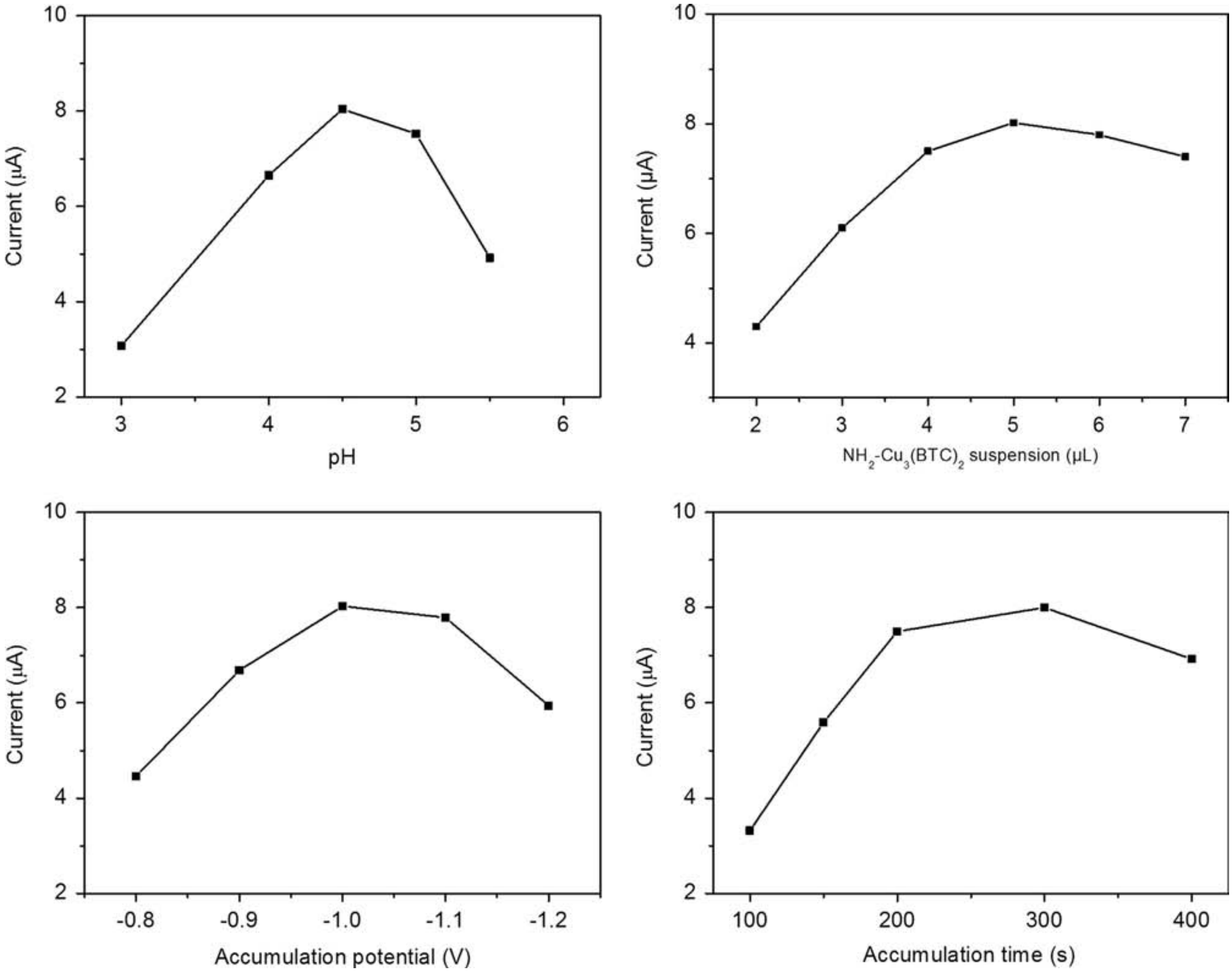

Fig. 4. Effects of pH, the amount of NH_2–$Cu_3(BTC)_2$ suspension, accumulation potential and accumulation time on the current intensity of lead.

Table 1
Comparison of this method for the determination of lead with other stripping techniques.

Electrode substrate	Method	Linear range (μmol L^{-1})	Detection limit (μmol L^{-1})	References
Diacetyldioxime carbon paste electrode	DPSV	0.1–15.0	0.01	[26]
Calixarenes/screen-printed carbon electrodes	DPSV	0.024–0.48	0.024	[27]
The renovated silver ring electrode	DPSV	0.001–0.1	0.0002	[28]
Hg-coated screen-printed electrode	SWSV	0.03–2.41	0.003	[29]
Poly(propylene imine) dendrimer/exfoliated graphite electrode	SWSV	2.5–40.0	0.83	[30]
Imidazole-functionalized polyaniline glassy carbon electrode	DPSV	0.01–1000	0.097	[31]
Amberlite IR-120 carbon paste electrode	DPSV	0.096–1.7	0.021	[32]
Mercury nano-droplets/screen-printed electrode	SWSV	0.04–0.2	0.023	[33]
Hybrid mesoporous silicas carbon paste electrode	ADSV	0.024–0.48	0.0012	[34]
Poly(diphenylamine-co-2-aminobenzonitrile) film glassy carbon electrode	DPSV	1.25–283	0.8	[35]
Salicylic acid modified glassy carbon electrode	DPSV	1–10	0.18	[36]
Montmorillonite calcium carbon paste electrode	DPSV	0.025–2	0.006	[37]
NH_2–$Cu_3(BTC)_2$ glassy carbon electrode	DPSV	0.01–0.5	0.005	This work

DPSV: differential pulse stripping voltammetry; ADSV: adsorptive stripping voltammetry; SWSV: square wave stripping voltammetry.

on the stripping current of lead was changed from 100 to 400 s (Fig. 4d). The peak current increased with the accumulation time increasing up to 300 s. It was probably owing to the interaction between the lead and the active sites of the modified electrode. When the accumulation time exceeded 300 s, the peak current decreased gradually. Taking into account both the sensitivity and efficiency, an accumulation period of 300 s was employed in the experiments.

3.3. The interferences

In order to assess the suitability of the developed procedure in analyzing real samples and demonstrate the selectivity of this new method for the determination of lead. Various amounts of potential species were added to a buffer solution containing 1.0×10^{-7} mol L^{-1} of lead, and the recommended method for sample analysis was employed. The tolerable concentration was taken as the measured signal variation ±5.0% relative error. The results show that Cd^{2+} (30-fold molar excess), Hg^{2+} (60-fold molar excess), Ni^{2+}, Co^{2+}, Zn^{2+} (100-fold molar excess), Al^{3+}, Bi^{2+} (300-fold molar excess), Mn^{2+}, Sn^{2+} (350-fold molar excess), Ag^{+}, Cr^{3+}, Fe^{3+} (500-fold molar excess), Cu^{2+}, Mg^{2+}, Ca^{2+}, K^{+}, Na^{+}, NO_3^-, Cl^-, SO_4^{2-} (at least 1000-fold molar excess) have negligible effect on the determination of lead. The above results indicated that the developed method is appropriate for the analysis of lead in real samples.

3.4. Analytical performances and method validation

Under the optimal conditions, the analytical performance of the proposed method for the determination of lead with a NH_2–$Cu_3(BTC)_2$ modified electrode was evaluated. The response was linear in the concentration range from 1.0×10^{-8} to 5.0×10^{-7} mol L^{-1} (R^2=0.9951). Regression equation of the calibration curves was i_p =6.3161+0.1411 C (i_p: μA, C: 10^{-8} mol L^{-1}). The limit of detection (LOD) was calculated from $3S_b/S$, where S_b is the standard deviation of 1.0×10^{-8} mol L^{-1} measurement (n=11) and S is the slope of linearity. The LOD was found to be 5.0×10^{-9}. As for the precision of measurement, a series of 11 repetitive measurements of solutions containing 1.0×10^{-8} mol L^{-1} target metals on the same electrode with 300 s accumulation time resulted in reproducible stripping peaks, with a relative standard deviation of 3.1%. Seven electrodes were fabricated under the same condition and their current responses towards 1.0×10^{-8} mol L^{-1} lead were examined. The RSD of the seven determinations was 5.6%. Moreover, the modified electrode can be repeatedly used up to 20 cycles without loss of analytical performance. These results indicate that NH_2–$Cu_3(BTC)_2$ modified electrode has good stability and repeatability, and could be used for lead measurements. We have compared this study with some other methods using different modified electrodes [36–37], and the results are shown in Table 1. It can be seen that the proposed method has relatively lower detection limit and good sensitivity. Furthermore, as novel porous crystalline materials, covalent strategy could be used for selective modification of MOFs surfaces, which will incorporate new functionalities into MOF synthesis and broaden the applications of MOFs based electrochemical sensor. To assess the applicability of the sensor, the NH_2–$Cu_3(BTC)_2$ modified electrode was employed to detect lead in certified standard samples (stream sediment and milk powder). The results are shown in Table 2. The concentration of lead in the sample were found to be 12.9 ± 1.8 and 0.06 ± 0.015 μg g^{-1}, respectively, which at 95% confidence level, are in good agreement with the certified values of 13.5 ± 2.3 and 0.07 ± 0.02 μg g^{-1}, confirming that this approach is of great accuracy and precision. In order to better demonstrate the usefulness of this detection method, we further analyzed the contents of lead in tap and lake water samples. The analytical results showed that satisfactory recoveries were listed in the range from 98 to 102 % (Table 3), which indicated that the proposed electrode was highly accurate, precise, and reproducible and can be used for direct analysis of lead in real samples.

Table 2
Validation of the method for the analysis of lead in certified reference materials.

Sample	Value[a] (μg g^{-1})	Found[a] (μg g^{-1})
Stream sediment	13.5 ± 2.3	12.9 ± 1.8
Milk powder	0.07 ± 0.02	0.06 ± 0.015

[a] Mean and standard deviation for 3 determinations.

4. Conclusion

In this work, novel electrode material named amino-functionalized metal-organic frameworks has been prepared by a simple one-pot method. XRD analysis revealed that the structure of $Cu_3(BTC)_2$ was not changed after amino-functionalization. The results indicated that the amino-functionalized metal-organic frameworks composite material could be used as a very suitable modifier for constructing an efficient and highly selective electrode for the determination of lead. NH_2–BDC linker formed stable complexes with lead at the solution/electrode interface and the complexed ions were reduced at the electrode surface in the subsequent accumulation step. The effects of different cations and anions on the determination of lead were investigated and found that the electrode is highly selective. The proposed chemically

Table 3
Determination of lead in different water samples.

Sample	Original[a] (× 10^{-8} mol L^{-1})	Spiked (× 10^{-8} mol L^{-1})	Found[a] (× 10^{-8} mol L^{-1})	Recovery (%)
Tap water	16.92 ± 1.20	1.00	17.91 ± 1.10	99
		5.00	22.01 ± 1.30	102
Lake water	45.16 ± 2.95	1.00	46.09 ± 3.02	93
		5.00	49.97 ± 3.81	96

[a] Mean and standard deviation for 3 determinations.

modified electrode was used in the determination of lead in certified standard reference materials and water samples.

Acknowledgments

This work was supported by the National Natural Science Foundation of China (21205103, 21275124), Jiangsu Provincial Nature Foundation of China (BK2012258), and a Project Funded by the Priority Academic Program Development of Jiangsu Higher Education Institutions.

References

[1] K.C. Honeychurch, J.P. Hart, D.C. Cowell, Anal. Chim. Acta 431 (2001) 89–99.
[2] R.L. Boeckx, Anal. Chem. 58 (1986) 274A–288A.
[3] M. Sperling, X.P. Yan, B. Welz, Spectrochim. Acta Part B 51 (1996) 1891–1908.
[4] Q. Zhou, N. Zhao, G. Xie, J. Hazard. Mater. 189 (2011) 48–53.
[5] J. Otero-Romaní, A. Moreda-Piñeiro, P. Bermejo-Barrera, A. Martin-Esteban, Talanta 79 (2009) 723–729.
[6] M.F. Philips, A.I. Gopalan, K.P. Lee, J. Hazard. Mater 237–238 (2012) 46–54.
[7] G. Raghu, S. Sampath, M. Pandurangappa, J. Solid State Electrochem. 16 (2012) 1953–1963.
[8] M. Mathew, S. Sureshkumar, N. Sandhyarani, Colloids Surf. B 93 (2012) 143–147.
[9] R. Sivasubramanian, M.V. Sangaranarayanan, Talanta 85 (2011) 2142–2147.
[10] E.A. Hutton, S.B. Hočevar, L. Mauko, B. Ogorevc, Anal. Chim. Acta 580 (2006) 244–250.
[11] W.W. Zhu, N.B. Li, H.Q. Luo, Talanta 72 (2007) 1733–1737.
[12] C.H. Xiong, H.Q. Luo, N.B. Li, J. Electroanal. Chem. 651 (2011) 19–23.
[13] P.A. Dimovasilis, M.I. Prodromidis, Anal. Chim. Acta 769 (2013) 49–55.
[14] Y. Ya, L. Mo, T. Wang, Y. Fan, J. Liao, Z. Chen, K.S. Manoj, F. Fang, C. Li, J. Liang, Colloids Surf. B 95 (2012) 90–95.
[15] C.T. Hsieh, H. Teng, W.Y. Chen, Y.S. Cheng, Carbon 48 (2010) 4219–4229.
[16] I. Ion, A.C. Ion, Sens. Actuators B 166–167 (2012) 842–847.
[17] S.S.Y. Chui, S.M.F. Lo, J.P.H. Charmant, A.G. Orpen, I.D. Williams, Science 283 (1999) 1148–1150.
[18] K. Schlichte, T. Kratzke, S. Kaskel, Microporous Mesoporous Mater. 73 (2004) 81–88.
[19] J. Mao, L. Yang, P. Yu, X. Wei, L. Mao, Electrochem. Commun. 19 (2012) 29–31.
[20] R. Senthil Kumar, S. Senthil Kumar, M. Anbu Kulandainathan, Electrochem. Commun. 25 (2012) 70–73.
[21] H. Hosseini, H. Ahmar, A. Dehghani, A. Bagheri, A.R. Fakhari, M.M. Amini, Electrochim. Acta 88 (2013) 301–309.
[22] H. Hosseini, H. Ahmar, A. Dehghani, A. Bagheri, A. Tadjarodi, A.R. Fakhari, Biosens. Bioelectron. 42 (2013) 426–429.
[23] O.G. Nik, X.Y. Chen, S. Kaliaguine, J. Membr. Sci. 413–414 (2012) 48–61.
[24] L.Y. Chen, C.L. Zhao, Z.D. Wei, S.N. Wang, Yang Gu, Mater. Lett. 65 (2011) 446–449.
[25] H. Dathe, E. Peringer, V. Roberts, A. Jentys, J.A. Lercher, C.R. Chimie 8 (2005) 753–763.
[26] C. Hu, K. Wu, X. Dai, S. Hu, Talanta 60 (2003) 17–24.
[27] K.C. Honeychurch, J.P. Hart, D.C. Cowell, D.W.M. Arrigan, Sens. Actuators B 77 (2001) 642–652.
[28] B. Baś, M. Jakubowska, Anal. Chim. Acta 615 (2008) 39–46.
[29] F. Fan, J. Dou, A. Ding, K. Zhang, Y. Wang, Anal. Sci. 29 (2013) 571–577.
[30] T. Ndlovu, O.A. Arotiba, S. Sampath, R.W. Krause, B.B. Mamba, J. Appl. Electrochem. 41 (2011) 1389–1396.
[31] P. Kumar, A. Joseph, P. Ramamurthy, S. Subramanian, Microchim. Acta 177 (2012) 317–323.
[32] M. Nascimento, P. Martelli, C. Furtado, A. Santos, L. Oliveira, H. Gorgulho, Microchim. Acta 173 (2011) 485–493.
[33] W. Song, L. Zhang, L. Shi, D.W. Li, Y. Li, Y.T. Long, Microchim. Acta 169 (2010) 321–326.
[34] A. Sánchez, S. Morante-Zarcero, D. Pérez-Quintanilla, I.D. Hierro, I. Sierra, J. Electroanal. Chem. 689 (2013) 76–82.
[35] M.F. Philips, A.I. Gopalan, K.P. Lee, J. Hazard. Mater. 237–238 (2012) 46–54.
[36] G. Raghu, S. Sampath, M. Pandurangappa, J. Solid State Electrochem. 16 (2012) 1953–1963.
[37] D. Sun, C. Wan, G. Li, K. Wu, Microchim. Acta 158 (2007) 255–260.